JMSR 1(1) (2025)

Journal of Material Science and Radiation

https://journals.balaipublikasi.id/jmsr

Safety Evaluation of MRI Magnetic Field Leakage from Different Configurations

Yap Siew Hong[1], Siti Aisyah Mohd Nordin[1], Mohd Mustajfa Awang Kechik[1*], Muhammad Khalis Abdul Karim[1], Zarina Ramli[2], Hussien Baqjiah[3], Soo Kien Chen[1], Kean Pah Lim[1], Muhammad Kashfi Shabdin[1], Aliah Nursyahirah Kamarudin[1], Aris Doyan[4], Arebat Ryad Alhadei Mohamed[1], Abdul Halim Shaari[1]

[1] Superconductor & Thin Films Laboratory, Department of Physics, Faculty of Science, Universiti Putra Malaysia, Malaysia.
[2] Clinical and Technical Support Sector, Family Health Development Division, Ministry of Health Malaysia, Putrajaya, Malaysia.
[3] Shandong Key Laboratory of Biophysics, Institute of Biophysics, Dezhou University, Shandong, China.
[4] Department of Physics Education, Faculty of Teacher and Education, University of Mataram, Lombok, Indonesia

Received: February 13, 2025
Revised: March 27, 2025
Accepted: April 25, 2025
Published: April 30, 2025

Corresponding Author:
Mohd Mustafa Awang Kechik
mmak@upm.edu.my

© 2025 The Authors. This open access article is distributed under a (CC-BY License)

Abstract: Magnetic Resonance Imaging (MRI) systems generate intense static magnetic fields (SMFs), with fringe field propagation varying considerably between installations, even among scanners that operate at the same nominal field strength. This study investigates the safety implications of magnetic field leakage by quantifying and comparing SMFs distributions surrounding multiple MRI facilities. The assessment covers 1.5 T MRI scanners at Hospital Canselor Tuanku Muhriz (HCTM) and Hospital Pakar Kanak-Kanak UKM (HPKK), and 3 T scanners at the National Cancer Institute / Institut Kanser Negara (IKN), Pusat Pengimejan Diagnostik Nuklear (PPDN), and HCTM. Magnetic field intensities were recorded using a Magnetometer HP-01 provided by the Medical Radiation Surveillance Division (BKRP), Ministry of Health Malaysia, and visualised using MATLAB to model spatial field dispersion. Statistical tools, including Box and Whisker plots and the Shapiro-Wilk test, were employed to analyse magnetic field uniformity and containment. Specifically, 1.5 T scanners at HCTM and HPKK, and 3.0 T scanners at IKN, PPDN, and HCTM, each displayed distinct SMFs propagation profiles. These findings align with earlier studies conducted in Italy, confirming that magnetic field distributions near the magnet core can differ substantially based on scanner model and site-specific installation variables—even when B_0 remains constant. Notably, HCTM exhibited superior SMFs confinement, with lower standard deviation and a narrower distribution range, suggesting better shielding design. This enhances occupational safety in zones where radiographers frequently operate. The results reinforce the need for site-specific SMFs assessments and optimised shielding practices to maintain safe MRI environments for both staff and patients.

Keywords: Magnetic field leakage; Magnetic field strength; Static magnetic fields.

Introduction

Magnetic Resonance Imaging (MRI) plays a pivotal role in modern medical diagnostics, offering unparalleled detail in imaging tissues, organs, and internal structures, such as the brain, spinal cord, and musculoskeletal system (Crawford et al., 2019; Holden et al., 2013; Mittendorff et al., 2022; Pradeep et al., 2022). Widely adopted in clinical practice, MRI operates through the use of superconducting materials to maintain a consistently powerful and uniform magnetic field, which remains active without interruption (Cross et al., 2018). Despite its advanced technology and widespread use, the full scope of risks related to MRI

How to Cite:
Hong, Y. S., Nordin, S. A. M., Kechik, M. M. A., Karim, M. K. A., Ramli, Z., Baqjiah, H., … Shaari, A. H. (2025). Safety Evaluation of MRI Magnetic Field Leakage from Different Configurations. *Journal of Material Science and Radiation*, *1*(1), 7–14. Retrieved from https://journals.balaipublikasi.id/index.php/jmsr/article/view/360

exposure remains inadequately understood (Pickup et al., 2019). This gap highlights the need for preliminary evaluations, particularly concerning magnetic field leakage (Panych & Madore, 2018; Shi et al., 2015; Vijayalaxmi et al., 2015; Yokoyama et al., 2020). MRI safety is a critical issue that cannot be overlooked, requiring constant attention and compliance with safety protocols by MR technologists and staff (Mittendorff et al., 2022). Ensuring a safe environment in the MRI room is essential, with strict adherence to operational guidelines to protect all individuals within the vicinity of the scanner.

MRI systems continuously operate, even during power failures, producing three types of magnetic fields: static, radiofrequency, and gradient fields (Hartwig et al., 2019). Of these, the static magnetic field, which ranges from 0.5 T to 11.7 T, plays a central role in generating detailed images by aligning hydrogen nuclei. However, the intense static field presents significant safety concerns, particularly the projectile risks associated with ferromagnetic objects drawn to the scanner. These objects can pose serious hazards due to both translational and rotational forces. Furthermore, the static magnetic field may interfere with medical devices that incorporate magnetic components, potentially causing malfunctions (Coskun, 2011; Durbridge, 2011; Schenck, 2000). Given these concerns, ensuring the MRI room's optimal design and operational procedures is essential for safeguarding both patients and personnel in clinical settings (Farrag, 2014).

The study of MRI safety concerning magnetic field leakage is critical for establishing safer MRI environments, particularly in countries such as the United States, Japan, and Italy, where there is a heightened awareness of the potential risks (Carr & Grey, 2002). These nations have invested in continuous research and safety protocols to mitigate the hazards associated with exposure to strong magnetic fields. In contrast, Malaysia lacks comprehensive research on this issue, and healthcare professionals are currently guided by legislation to perform necessary preventive work without fully understanding the risks. The U.S. Food and Drug Administration (FDA) has set the limit for static magnetic field strengths at 8 T for human use (Mittendorff et al., 2022), paving the way for ultra-high MRI systems, but the risk of magnetic field leakage persists, particularly as MRI systems grow more powerful. Recent increases in MRI-related accidents and injuries, including fatal incidents caused by the attraction of ferromagnetic objects, underscore the urgent need for better safety standards (Khazi et al., 2018). This study aims to address these gaps by evaluating MRI safety in Malaysian healthcare facilities and ensuring that effective safety measures are in place.

Ultimately, a significant knowledge gap exists between healthcare facility architecture and radiographers' requirements when planning MRI room layouts and safety protocols (Ayasrah, 2022; Gilk & Kanal, 2015). While the utility needs and room dimensions vary considerably based on the equipment, the focus is often on fitting the equipment into available space. The equipment supplier's goal is to ensure the machinery will fit, often overlooking future needs and function in the context of long-term safety. Therefore, effective MRI room design must consider both present and future safety requirements, ensuring the facility layout accommodates both current technology and evolving needs in MRI practice (Rathebe et al., 2021).

The primary objective of this study is to quantify the intensity of the magnetic fringe field from different MRI configurations using a magnetometer. The study has the following sub-objectives: i) to compare the magnetic fringe fields of different MRI configurations across various facilities, and ii) to evaluate which study area exhibits better distribution and confinement of the static magnetic field. The study focuses on MRI facilities at the National Cancer Institute (IKN), Pusat Pengimejan Diagnostik Nuklear (PPDN), Hospital Canselor Tuanku Muhriz (HCTM), and Hospital Pakar Kanak-Kanak UKM (HPKK). The magnetic field of each scanner was measured using a Magnetometer HP-01 borrowed from the Bahagian Kawalselia Radiasi Perubatan Ministry of Health Malaysia (BKRP MOH). Data was collected from 1.5 T MRI units in HPKK and HCTM, and 3 T MRI units in IKN, PPDN, and HCTM. The magnetic fringe fields were mapped using MATLAB, and statistical analyses, including Box and Whisker Plots and Paired T-Tests, were employed to compare the confinement of magnetic fields across the different MRI configurations. The findings aim to provide useful insights for MRI safety, particularly with regard to magnetic field leakage, contributing to a better understanding of MRI environments. The study's outcomes will be valuable for MRI facilities seeking to optimise room design and safety measures, especially as the demand for higher-powered MRI systems continues to grow.

Method

In this study, measurements of SMFs were carried out at four public hospitals in Malaysia to assess exposure levels around MRI scanners with field strengths of 1.5 T and 3.0 T. Spot measurements were used to represent exposure points, and the distance from each spot to the MRI machine was recorded. The research followed a descriptive, qualitative approach. Most data were collected from Zone IV, where the MRI machines are located, but Zones I to III were also included for a full overview of the magnetic environment. The MRI units included two 1.5 T scanners at Hospital Canselor Tuanku Muhriz (HCTM) and Hospital Pakar Kanak-Kanak UKM (HPKK), and three 3.0 T scanners at the National Cancer Institute (IKN), Pusat Pengimejan Diagnostik Nuklear (PPDN), and another at HCTM.

Measurements were taken using the HP-01 Magnetometer, placed one metre above the floor with the sensor facing the MRI unit. Distances were measured using a measuring tape. The selected points reflected where typical MRI activities take place. Each reading was taken over three minutes, and the final result was recorded using the hold function of the device. All values were saved in a text document for later analysis.

A key part of this research involved visualising the SMFs using MATLAB. A custom script was used to generate 3D images showing the strength and spread of the magnetic field within the MRI rooms. MATLAB's ability to manage data, create visualisations, and support coding made it well-suited to this task. The study had discussed the 3d mapping in more detail, comparing the magnetic field distribution in the 1.5 T and 3.0 T systems using statistical analysis.

Statistical Analysis

The SMFS data were analysed using both visual and statistical methods. Box and whisker plots in Excel were used to show how the magnetic field levels varied across the different MRI systems. The Shapiro-Wilk test in S Statistical Package for the Social Sciences (SPSS) checked whether the data followed a normal distribution, confirming if parametric tests could be used.

Statistical Package for the Social Sciences (SPSS)

SPSS, developed by IBM, is a tool used for statistical analysis. In this study, it was used to organize the data, calculate key statistics, and perform further testing.

Paired t-test

A paired t-test was used to compare the average SMF readings from different MRI scanners. This helped identify which machines had better magnetic field control, reducing the risk of field leakage into nearby areas.

Results and Discussion

Static Magnetic Field Distributions

Static magnetic field intensities were assessed at predetermined positions around the MRI scanners. To determine whether the levels adhered to occupational exposure standards, the average exposure values obtained from five separate MRI systems were compared against the limits set by the International Commission on Non-Ionizing Radiation Protection (ICNIRP). A summary of the average exposure levels recorded at various points is presented in Tables 1 and 2, providing a comprehensive breakdown of SMFs emissions recorded from both 3.0 T and 1.5 T MRI systems.

Table 1. The measured values of SMFs s exposure from 3 T scanners in IKN, PPDN, and HCTM

Locations	Sampling Position	Total Mean ± SD (mT)	Minimum (mT)	Maximum (mT)	COV_{tot} (%)
IKN	Left side gantry (inside 5G line) (L1)	0.224 ± 0.011	0.209	0.239	4.46
	Left side gantry (outside 5G line) (L2)	0.257 ± 0.007	0.241	0.264	2.33
	Left extremities (L3)	4.85 ± 0.004	4.843	4.856	0.08
	Right extremities (L4)	7.707 ± 0.395	7.053	7.952	5.13
	Right side gantry (inside 5G line) (L5)	28.418 ± 0.007	28.406	28.428	0.02
	Right side gantry (outside 5G line) (L6)	18.444 ± 0.007	18.429	18.449	0.04
	Back side gantry (L7)	84.900 ± 0.316	84.000	85.000	0.38
	Right side gantry (above L6) (L8)	43.422 ± 0.011	43.413	43.436	0.03
PPDN	Left side gantry (inside 5G line) (L1)	2.961 ± 2.245	2.25	4.325	0.76
	Left side gantry (outside 5G line) (L2)	2.524 ± 0.342	2.254	3.926	0.14
	Left extremities (L3)	2.945 ± 1.127	1.72	4.234	0.38
	Right extremities (L4)	5.221 ± 0.856	3.49	7.749	16.40
	Right side gantry (inside 5G line) (L5)	15.146 ± 1.73	10.575	20.337	11.42
	Right side gantry (outside 5G line)(L6)	4.125 ± 0.927	3.630	7.646	22.47
	Back side gantry (L7)	165.640 ± 0.628	162.800	166.300	0.38
HCTM	Left side gantry (inside 5G line) (L1)	1.129 ± 1.672	0.319	9.572	1.48
	Left side gantry (outside 5G line) (L2)	1.403 ± 1.526	0.306	6.619	1.08
	Left extremities (L3)	6.722 ± 10.172	0.590	44.311	1.51
	Right extremities (L4)	6.473 ± 9.102	0.414	42.577	1.41
	Right side gantry (inside 5G line) (L5)	9.212 ± 10.724	1.263	49.793	1.16
	Right side gantry (outside 5G line) (L6)	2.633 ± 2.970	0.302	12.381	1.13

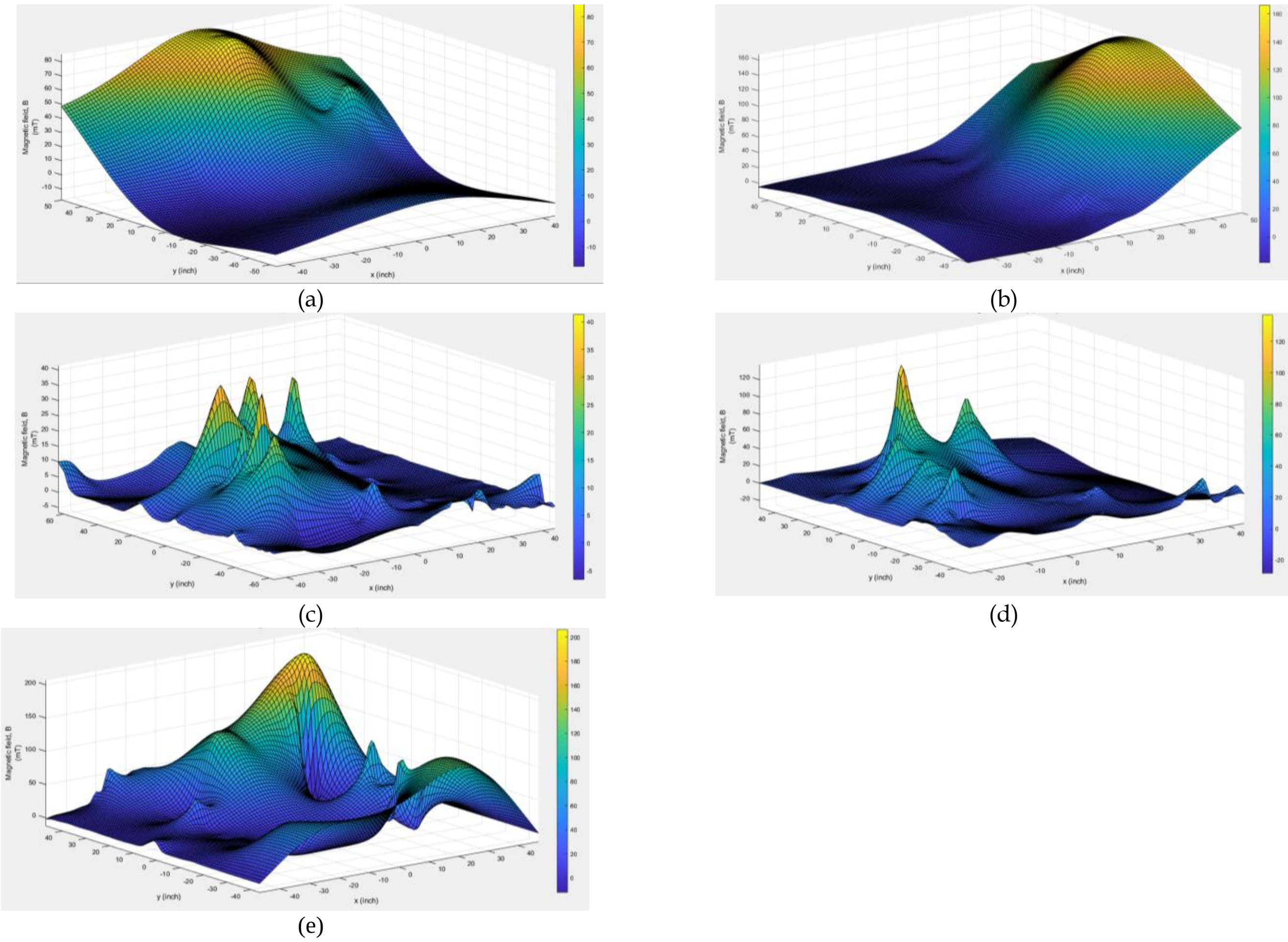

Figure 1. Static Magnetic Field around: (a) 3 T scanner in IKN; (b) 3 T scanners in PPDN; (c) 3 T scanner in HCTM; (d) 1.5 T scanner in HCTM; and (e) 1.5 T scanner in HPKK

Table 2. The measured values of SMFs s exposure from 1.5 T scanners in HCTM and HPKK

Locations	Sampling Position	Total Mean ± SD (mT)	Minimum (mT)	Maximum (mT)	COV $_{tot}$ (%)
HCTM	Left extremities (L1)	0.687 ± 0.696	0.032	2.876	1.01
	Left side gantry (L2)	23.84 ± 31.141	0.555	104.000	1.31
	Left brain (L3)	7.500 ± 5.089	1.633	22.211	0.68
	Right brain (L4)	15.500 ± 36.97	0.707	145.000	2.38
	Right side gantry (L5)	14.783 ± 19.435	0.539	75.000	1.31
	Right extremities (L6)	17.536 ± 24.602	0.695	58.000	1.40
	Front left extremities (L7)	4.527 ± 4.640	0.113	13.093	1.02
	Front right extremities (L8)	5.857 ± 7.806	0.072	30.549	1.33
HPKK	Left extremities (L1)	43.152 ± 54.940	0.441	131.000	1.27
	Left side gantry (L2)	19.483 ± 34.505	0.587	26.889	1.77
	Left brain (L3)	22.402 ± 12.681	4.000	34.175	0.56
	Right brain (L4)	18.338 ± 15.345	1.115	36.708	0.84
	Right side gantry (L5)	7.522 ± 11.824	0.773	53.000	1.57
	Right extremities (L6)	18.933 ± 35.030	1.513	121.000	1.85
	Front left extremities (L7)	27.480 ± 31.941	1.449	134.000	1.16
	Front right extremities (L8)	6.720 ± 8.469	0.997	38.000	1.26

These Table 1, include key statistical indicators such as mean values, standard deviations, maximum and minimum field strengths, as well as the coefficient of variation. Notably, the 3.0 T machines exhibited a broader spread in data, as reflected by their higher coefficients of variation, indicating greater inconsistency in field intensity around the average. All recorded values for both scanner strengths were found to be statistically significant, with p-values less than 0.01.

In the 3.0 T systems, the most intense SMFs emissions were consistently recorded at the rear section of the gantry, particularly in the cranial region. Specifically, measurements showed 84.900 ± 0.316 mT in IKN, 165.640 ± 0.628 mT in PPDN, and 9.212 ± 10.724 mT in HCTM. In contrast, the 1.5 T units revealed a different emission profile (Table 2), where the highest SMFs levels were observed on the right side of the cranial region (L5) in HCTM (15.500 ± 36.970 mT, with a peak of 145.000 mT) and at the left anterior limb region (27.480 ± 31.941 mT, peaking at 134.000 mT). Interestingly, despite being a lower-strength scanner, the 1.5 T system in HPKK demonstrated notably elevated field emissions, averaging 43.152 ± 54.940 mT, as outlined in Table 2.

Each measurement location was monitored continuously, capturing real-time SMFs intensity every second over an approximate period of three minutes. The spatial distribution of these fields within the MRI suites, surrounding both the 1.5 T and 3.0 T systems, was then visualised in three dimensions. This representation, displayed in Figures 1 to 5, was produced using a custom MATLAB script designed to model the SMFs layout throughout the scanner environment. From the findings, it is evident that the SMFs intensity peaks in the vicinity of the scanner's central axis at coordinates (0, 0). This outcome suggests that the magnetic shielding, intended to maintain field uniformity within the magnet's core, inadvertently results in elevated SMFs levels around the patient table and near the gantry area. Notably, these zones correspond to the primary working positions of radiographers during patient setup, thereby subjecting them to full-body exposure to the magnetic field.

Comparison of SMFs Emission from 1.5 Scanner

A comparative analysis of SMFs intensities was conducted between two separate 1.5 T MRI systems installed at HCTM and HPKK. To evaluate whether the variations in exposure levels across the designated measurement points were statistically meaningful, the Shapiro-Wilk test was employed as a parametric assessment tool. The results indicated statistically significant disparities at all measured distances from the central reference point, with p-values recorded below 0.001.

The data sets collected from the respective facilities exhibit distinct patterns of dispersion that appear influenced by more than just their physical location. As illustrated in Figures 2 (a) and (b), the box and whisker plot for HCTM reveals a notably more balanced distribution, suggesting greater uniformity in the magnetic environment. This could be attributed to the presence of more effective shielding within HCTM's MRI suite. In contrast, HPKK's plot—particularly for the L1 position—displays a pronounced left skew, with a distribution span nearly four times broader than that of HCTM, potentially raising concern considering the paediatric nature of patients at HPKK.

At the L1 coordinate, HCTM exhibits a symmetrical distribution, in contrast to the skewness observed in HPKK. For the L2 position, both distributions appear skewed to the left, although HCTM's spread remains notably more compact, and a possible 11% difference is observed between the two. At L3 and L4, a similar pattern continues, where HPKK displays box lengths roughly double those of HCTM, again skewed to the left. On L5, the median recorded at HCTM aligns closely with the upper adjacent line of HPKK's range, and at L8, both institutions show comparable data distributions.

What distinguishes the two settings is not the median—which remains largely overlapping—but rather the concentration and dispersion of recorded values. In several cases, outliers identified within HCTM are still relatively close to HPKK's upper bound, indicating tighter field control. These findings suggest superior SMFs containment within HCTM, supported by its narrower range and reduced standard deviation. Overall, the data point to a more homogeneous magnetic field environment in HCTM's MRI room, which may enhance both operational safety and patient protection.

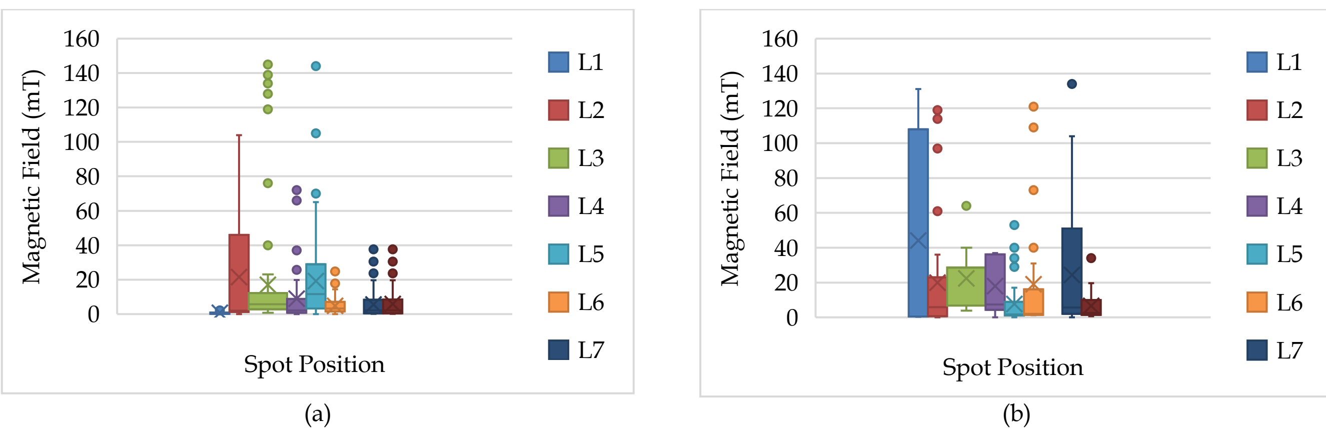

Figure 2. Boxplot of SMFs in: (a) HCTM; and (b) HPKK.

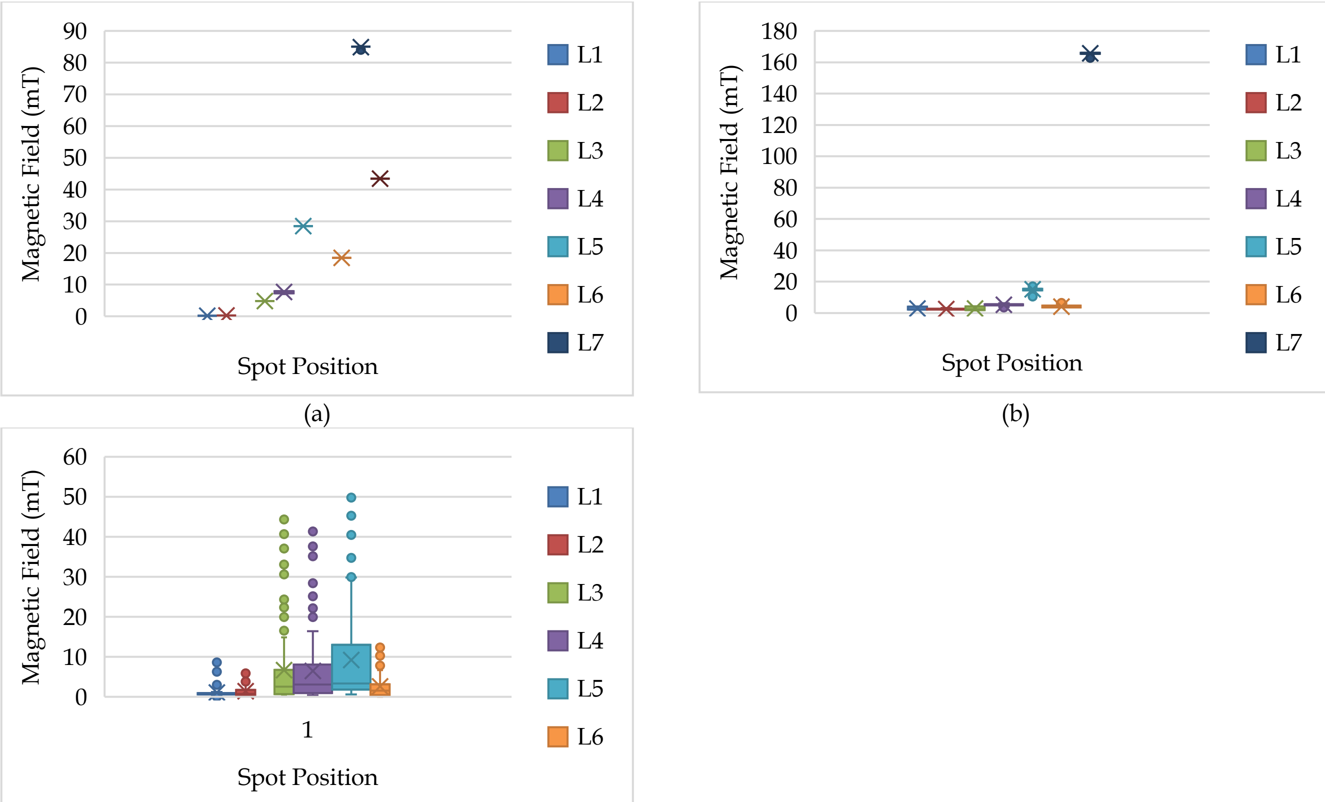

(a) (b) (c)

Figure 3. Boxplot of SMFs in: (a) IKN; (b)PPDN; and (c) HCTM.

Comparison of SMFs Emission from 3 T Scanner

To investigate the variation in magnetic field exposure across multiple scanner positions, the Shapiro-Wilk test was employed using data acquired during active scanning sessions at IKN (Figure 3a), PPDN (Figure 3b) and HCTM (Figure 3c). Refer Figure 3a, at the initial measurement point on the left flank of the gantry (L1), statistical outcomes varied—IKN reported a non-significant result (p = 0.524), whereas HCTM approached the threshold of significance (p = 0.056). Further along the gantry's left side, beyond the 5-gauss boundary (L2), both IKN and HCTM reflected no meaningful differences in exposure levels, while PPDN produced a significant variation (p = 0.01). In the area corresponding to the patient's left extremities (L3), contrasting trends were noted: IKN showed consistent exposure levels with no statistical significance, whereas both HCTM and PPDN indicated notable differences ($p < 0.01$). Measurements from the right extremity (L4) revealed that only IKN displayed significant variation ($p < 0.001$); no such difference was recorded for HCTM or PPDN. On the right-hand side of the gantry, within the 5G threshold (L5), all three facilities—IKN, PPDN, and HCTM—exhibited no statistically significant deviation in field strength. However, moving outside this boundary to position L6, both IKN and HCTM demonstrated significant discrepancies ($p < 0.01$). Finally, at the rear of the gantry (L7), a strong statistical difference was identified at IKN ($p < 0.001$), further emphasising positional sensitivity in SMFs distribution across the scanning environment.

Conclusion

This study presents a detailed evaluation of SMFs emissions surrounding 1.5 T and 3.0 T MRI systems across multiple clinical settings. All SMFs exposure levels recorded were statistically significant and fell within the occupational safety limits set by the ICNIRP. Greater variation in field intensity was observed around the 3.0 T systems, especially at the rear of the gantry, whereas the 1.5 T scanners showed more widespread emissions, with peaks noted near the cranial and limb regions. Importantly, the findings reveal that the propagation patterns of SMFs differed across all sites, despite the scanners sharing the same nominal magnetic field strength (B_0). Specifically, 1.5 T scanners at HCTM and HPKK, and 3.0 T scanners at IKN, PPDN, and HCTM, each displayed unique spatial distributions. These results are consistent with previous research conducted in Italy, which demonstrated that, although nominal B_0 values remain constant, the magnetic field distributions near the core magnet can vary significantly depending on scanner model and site-specific installation factors. Comparative analysis of SMFs containment between facilities further highlighted HCTM's superior shielding performance, resulting in tighter field distribution, lower standard deviation, and improved homogeneity. These factors are critical in reducing occupational exposure, particularly in areas near the bore where radiographers routinely operate. In conclusion, the study underscores the need for site-specific magnetic field assessments and optimised shielding design to ensure consistent safety and performance in MRI environments.

Acknowledgments
Authors gratefully acknowledge financial support from the Ministry of Higher Education Malaysia (MOHE) for Fundamental Research Grant Scheme FRGS/1/2024/STG05/UPM/02/4 (5540701) Universiti Putra Malaysia.

Author Contributions
Conceptualization, Mohd Mustafa Awang Kechik and Siti Aisyah Mohd Nordin; methodology, Siti Aisyah Mohd Nordin; software, Mohd Mustafa Awang Kechik, Soo Kien Chen and Kean Pah Lim; validation, Arebat Ryad Alhadei Mohamed, Hussien Baqiah, Soo Kien Chen, Kean Pah Lim and Abdul Halim Shaari; formal analysis, Siti Aisyah Mohd Nordin; investigation, Siew Hong Yap and Siti Aisyah Mohd Nordin; resources, Mohd Mustafa Awang Kechik, Soo Kien Chen and Kean Pah Lim; data curation, Siew Hong Yap, Aliah Nursyahirah Kamarudin and Siti Aisyah Mohd Nordin; writing—original draft preparation, Siew Hong Yap.; writing—review and editing, Siew Hong Yap, Aris Doyan, Aliah Nursyahirah Kamarudin and Zarina Ramli; visualization, Soo Kien Chen, Muhammad Kashfi Shabdin, Muhammad Khalis Abdul Karim , and Abdul Halim Shaari; supervision, Mohd Mustafa Awang Kechik; project administration, Mohd Mustafa Awang Kechik; funding acquisition, Mohd Mustafa Awang Kechik. All authors have read and agreed to the published version of the manuscript.

Funding
This research was funded by Ministry of Higher Education Malaysia (MOHE) for Fundamental Research Grant Scheme FRGS/1/2024/STG05/UPM/02/4 Universiti Putra Malaysia, grant number 5540701

Conflicts of Interest
The funders had no role in the design of the study; in the collection, analyses, or interpretation of data; in the writing of the manuscript; or in the decision to publish the results.

References

Ayasrah, M. (2022). MRI Safety Practice Observations in MRI Facilities Within the Kingdom of Jordan, Compared to the 2020 Manual on MR Safety of the American College of Radiology. *Medical Devices: Evidence and Research*, *15*(null), 131-142. https://doi.org/10.2147/MDER.S360335

Carr, M. W., & Grey, M. L. (2002). Magnetic Resonance Imaging: Overview, risks, and safety measures. *AJN The American Journal of Nursing*, *102*(12), 26-33. Retrieved from https://journals.lww.com/ajnonline/fulltext/2002/12000/magnetic_resonance_imaging__overview,_risks,_and.12.aspx

Coskun, O. (2011). Magnetic resonance imaging and safety aspects. *Toxicology and Industrial Health*, *27*(4), 307-313. https://doi.org/10.1177/0748233710386413

Crawford, R. J., Fortin, M., Weber, K. A., Smith, A., & Elliott, J. M. (2019). Are Magnetic Resonance Imaging Technologies Crucial to Our Understanding of Spinal Conditions? *Journal of Orthopaedic & Sports Physical Therapy*, *49*(5), 320-329. https://doi.org/10.2519/jospt.2019.8793

Cross, N. M., Hoff, M. N., & Kanal, K. M. (2018). Avoiding MRI-Related Accidents: A Practical Approach to Implementing MR Safety. *Journal of the American College of Radiology*, *15*(12), 1738-1744. https://doi.org/10.1016/j.jacr.2018.06.022

Durbridge, G. (2011). Magnetic Resonance Imaging: Fundamental Safety Issues. *Journal of Orthopaedic & Sports Physical Therapy*, *41*(11), 820-828. https://doi.org/10.2519/jospt.2011.3906

Farrag, S. I. (2014, 8-10 Dec. 2014). A numerical computational method of MRI static magnetic field for an ergonomic facility design guidelines. 2*014 IEEE Conference on Biomedical Engineering and Sciences (IECBES)*. https://doi.org/10.1109/IECBES.2014.7047595.

Gilk, T., & Kanal, E. (2015). Planning an MR suite: What can be done to enhance safety? *Journal of Magnetic Resonance Imaging*, *42*(3), 566-571. https://doi.org/10.1002/jmri.24794

Hartwig, V., Biagini, C., De Marchi, D., Flori, A., Gabellieri, C., Virgili, G., Ferrante Vero, L. F., Landini, L., Vanello, N., & Giovannetti, G. (2019). The Procedure for Quantitative Characterization and Analysis of Magnetic Fields in Magnetic Resonance Sites for Protection of Workers: A Pilot Study. *Annals of Work Exposures and Health*, *63*(3), 328-336. https://doi.org/10.1093/annweh/wxz002

Holden, R. J., Pascale, C., P., G. A., Peter, H., Schoofs, H. A., Ant, O. A., & and Rivera-Rodriguez, A. J. (2013). SEIPS 2.0: a human factors framework for studying and improving the work of healthcare professionals and patients. *Ergonomics*, *56*(11), 1669-1686. https://doi.org/10.1080/00140139.2013.838643

Khazi, S., Shetty, S., Reddy, S., Vannala, V., Shetty, R., & Shetty, P. (2018). Magnetic resonance imaging mishaps: A brief review. *Journal of Datta Meghe Institute of Medical Sciences University*, *13*, 160. https://doi.org/10.4103/jdmimsu.jdmimsu_63_18

Mittendorff, L., Young, A., & Sim, J. (2022). A narrative review of current and emerging MRI safety issues: What every MRI technologist (radiographer) needs to know. *Journal of Medical Radiation Sciences*, *69*(2), 250-260. https://doi.org/10.1002/jmrs.546

Panych, L. P., & Madore, B. (2018). The physics of MRI safety. *Journal of Magnetic Resonance Imaging*, *47*(1), 28-43. https://doi.org/10.1002/jmri.25761

Pickup, L., Nugent, B., & Bowie, P. (2019). A preliminary ergonomic analysis of the MRI work system environment: Implications and recommendations for safety and design. *Radiography*, *25*(4), 339-345. https://doi.org/10.1016/j.radi.2019.04.001

Pradeep, D., Tembhre, M. K., Parihar, A. S., & Rao, C. (2022). Chapter 4 - Magnetic resonance imaging: Basic principles and advancement in clinical and diagnostics approaches in health care. In M. Suar, N. Misra, & N. S. Bhavesh (Eds.), *Biomedical Imaging Instrumentation* (pp. 45-66). Academic Press. https://doi.org/10.1016/B978-0-323-85650-8.00005-X

Rathebe, P., Weyers, C., & Raphela, F. (2021). Exposure levels of radiofrequency magnetic fields and static magnetic fields in 1.5 and 3.0 T MRI units. *SN Applied Sciences*, *3*(2), 157. https://doi.org/10.1007/s42452-021-04178-3

Schenck, J. F. (2000). Safety of Strong, Static Magnetic Fields. *Journal of Magnetic Resonance Imaging*, *12*(1), 2-19. https://doi.org/10.1002/1522-2586(200007)12:1

Shi, Y., Zhang, C., Li, R., Cai, M., & Jia, G. (2015). Theory and Application of Magnetic Flux Leakage Pipeline Detection. *Sensors*, *15*(12), 31036-31055. Retrieved from https://www.mdpi.com/1424-8220/15/12/29845

Vijayalaxmi, Fatahi, M., & Speck, O. (2015). Magnetic resonance imaging (MRI): A review of genetic damage investigations. *Mutation Research/Reviews in Mutation Research*, *764*, 51-63. https://doi.org/10.1016/j.mrrev.2015.02.002

Yokoyama, S., Miura, H., Matsuda, T., Inoue, T., Morita, Y., Eguchi, R., Otake, S., Tanabe, H., Sato, S., Kiss, T., Miyagi, D., Tsuda, M., Nakamura, T., & Shirai, Y. (2020). Design and Cooling Properties of High Stable Field REBCO Superconducting Magnet for MRI. *IEEE Transactions on Applied Superconductivity*, *30*(4), 1-4. https://doi.org/10.1109/TASC.2020.2973936